

**DESIGN, SYNTHESIS AND CHARACTERIZATION
OF 4-OXOBUTANOIC ACID ANALOGUES AS
POTENTIAL HUMAN HYPOXIA INDUCIBLE
FACTOR (HIF) PROLYL HYDROXYLASE
DOMAIN 2 (PHD-2) INHIBITORS**

by

CHONG MUI PHIN

**Thesis submitted in fulfilment of the requirements
for the degree of
Master of Science**

September 2018

ACKNOWLEDGEMENT

First of all, I am highly thankful to the State Government of Sabah for granting me a full time scholarship to pursue my Master of Science (Chemistry) at Universiti Sains Malaysia (USM). The contribution of State Government of Sabah will greatly help me develop and succeed in my future endeavours.

In addition, it is my utmost pleasure to acknowledge and extend my intense gratitude and deep regards to my supervisor, Dr. Yeoh Kar Kheng who gave me an opportunity to complete this research project under his supervision, giving me vital encouragement and monitoring throughout the course of this study.

My deepest appreciation and gratitude also goes to Prof. Habibah A. Wahab and her students, Dr. Muhammad Yusuf and Dr. Maywan Horiono for their guidance on computational work. Not only that, my gratitude also goes to Cheah June Sun who have guided me in this study.

I also wish to extend my loving thanks to all of the lecturers and science officers of the School of Chemical Sciences for their kind help, support, patience and friendship. My deepest apologies for missing out anybody in my acknowledgement.

Last but not least, my heartfelt thanks to my parents and family members for their care and patience. They have supported me in every way possible during ups and downs in my life. My parents especially have been selfless in giving me the best of everything. Words cannot express my sincere gratefulness for their constant encouragement and love.

TABLE OF CONTENTS

Acknowledgement	ii
Table of Contents	iii
List of Tables	vii
List of Figures	viii
List of Schemes	xiv
List of Abbreviations and Symbols	xv
Abstrak	xvii
Abstract	xviii

CHAPTER 1 INTRODUCTION AND LITERATURE REVIEW

1.1 Hypoxia	1
1.2 Hypoxia Inducible Factor (HIF)	1
1.3 Hypoxia signaling pathway	3
1.4 Prolyl Hydroxylase Domain (PHDs)	6
1.5 Prolyl Hydroxylase Domain (PHDs) inhibitors	9
1.5.1 Iron chelator	9
1.5.2 Divalent transition metal ions	9
1.5.3 2-OG competitive prolyl hydroxylase domain inhibitors	10

1.5.4	Dual-action prolyl hydroxylase domain inhibitors	13
1.6	Therapeutic Uses of Prolyl Hydroxylase Domain Inhibitors	15
1.7	Amide Bond and Prolyl Hydroxylase Domain Inhibitors	16
1.8	Computer Aided Drug Design (CADD)	18
1.9	Problem Statement	21
1.10	Research Objectives	22
 CHAPTER 2 MATERIALS AND METHODS		
2.1	Chemicals and Solvents	23
2.2	General Experimental Procedures	23
2.2.1	Reaction Monitoring	23
2.2.2	Isolation and Purification	24
2.2.2(a)	Column chromatography	24
2.2.2(b)	Recrystallization	24
2.2.3	Characterization of compounds	24
2.2.3(a)	Nuclear Magnetic Resonance Spectroscopy (NMR)	25
2.2.3(b)	Fourier Transform Infrared Spectroscopy (FT-IR)	25
2.2.3(c)	Elemental Analysis	25
2.2.3(d)	Direct Infusion Mass Spectrometry (DI-MS)	25
2.2.3(e)	Melting Point Determination	26

2.3	Computer Aided Drug Design	26
2.3.1	Ligands Generation and Optimization	26
2.3.2	Molecular docking studies	26
2.3.2(a)	Protein preparation	27
2.3.2(b)	Positive control docking	27
2.3.2(c)	Ligands-protein docking	27
2.3.2(d)	Ligands-protein visualization	28
2.4	PHD-2 RapidFire Assay (RF-MS)	28
2.5	Synthesis of 4-Oxobutanoic Acid Analogues	29
 CHAPTER 3 RESULTS AND DISCUSSION		
3.1	Inhibitor Design	42
3.2	Molecular Docking Studies	43
3.2.1	Positive control docking	43
3.2.2	Free energy of binding	45
3.2.3	Docked conformation	46
3.3	Reaction of Primary Amine With Succinic Anhydride	62
3.4	Reaction of Sulfonamide with Succinic Anhydride	65
3.5	Characterization of 4-Oxobutanoic Acid Analogues	67
3.6	<i>In vitro</i> PHD-2 Inhibitory Studies of 4-Oxobutanoic Analogues	140

CHAPTER 4 CONCLUSION	149
REFERENCES	152
APPENDICES	

LIST OF TABLES

		Page
Table 1.1	The IC ₅₀ values of various divalent transition metal ions against PHD-2 (Sekirnik <i>et al.</i> , 2005).	10
Table 1.2	The reported IC ₅₀ values of 2-OG competitive inhibitors against PHD-2	11
Table 1.3	The IC ₅₀ of values of diacylhydrazine-based dual-action inhibitors in PHD-2 active site.	14
Table 3.1	The free binding energy of 4-oxobutanoic acid analogues estimated by Autodock 4.2	45
Table 3.2	The melting point determination, elemental analysis, DIMS and FT-IR of 4-oxobutanoic acid analogue compounds	68
Table 3.3	¹ H NMR (500 MHz, δ _H) and ¹³ C NMR (125 MHz, δ _C)	70
Table 3.4	The half-maximal inhibitory concentration (IC ₅₀) of 4-oxobutanoic acid analogue compounds as PHD-2 inhibitor. ND, not determined.	141

LIST OF FIGURES

	Page
Figure 1.1	2
<p>Schematic sketching of HIF isoform: (a) HIF-1α. (b) HIF-1β. Abbreviations for N-TADN and C-TAD: Amino-terminal and carboxy-terminal transactivating domains; b-HLH: Basic helix loop-helix for DNA binding; PAS A and Pas B: Protein domain critical for dimerization. At the end of structure, the total number of amino acids for each subunit were labelled. (Figure reviewed from Hellwig-Bürgel, 2009; Ke and Costa, 2006; Semenza <i>et al.</i>, 1998)</p>	
Figure 1.2	4
<p>HIF prolyl hydroxylases (PHDs) and Factor inhibiting HIF (FIH) utilizing ferrous ion (Fe²⁺), 2-oxoglutarate (2-OG) and oxygen (O₂) as cofactor/co-substrate to catalyze hydroxylation, forming hydroxy-proline/asparagine residue, succinate and carbon dioxide (Epstein <i>et al.</i>, 2001; McDonough <i>et al.</i>, 2006)</p>	
Figure 1.3	4
<p>The HIF transcriptional pathway: oxygen sensing and signaling under normoxic and hypoxic conditions by PHDs and FIH (Yan <i>et al.</i>, 2010).</p>	
Figure 1.4	8
<p>Sequence alignment of Human PHD-1, PHD-2 and PHD-3. (a) Residues shaded with black were highly conserved sequence similarities. (b) Ribbon presentation of crystallographic PHD-2 (cyan and violet) in complex with 8-iodo bicyclic isoquinoline (yellow) and iron (pink). The eight major β-strands of DSBH are highlighted in violet and numbered (βI-βVIII) and α-helices in cyan (α1-α4).</p>	
Figure 1.5	17
<p>Three known types of amide (a) carboxamide (b) sulfonamide (c) phosphoramidate.</p>	
Figure 1.6	20
<p>The progress of discovering drug candidates using CADD. (M Hassan <i>et al.</i>, 2016).</p>	
Figure 3.1	44
<p>In the PHD2 structure (beige), BIQ extracted from the crystal structure (violet) and re-docked BIQ (green) were superimposed, chelate the metal ferrous ion (cyan) through the nitrogen (blue) and oxygen (red) atom, resulting the formation of coordination bond and are represented by black dashed line. Only related active site residues (magenta) were showed. (PDB ID: 2HBT).</p>	
Figure 3.2	47
<p>The docked conformation of compound F1a in PHD2.Fe(II) complex. Compound F1a chelates the ferrous ion (cyan)</p>	

through its benzothiazole ring nitrogen (blue) atom (N-Fe[II]; 2.3 Å) and its carbonyl oxygen (red) (O-Fe[II]; 1.5Å). The formation of hydrogen bond through the carboxylate oxygen and active site protein residue (magenta) (O-Arg383; 1.8Å and 1.9Å; O-Tyr329; 1.8Å). (b) Superimposition of compound F1a and BIQ in PHD2.Fe(II) in the comparably narrow slot-shaped active site pocket.

- Figure 3.3 (a) The docked conformation of compound F1b in PHD2.Fe(II) complex. Compound F1b chelates the ferrous ion (cyan) through its benzothiazole ring sulphur atom (yellow) (S-Fe[II]; 3.2 Å) and carbonyl oxygen (red) (O-Fe[II]; 1.6 Å). The formation of hydrogen bond through the carboxylate oxygen and active site protein residue (magenta) (O-Arg383; 2.1 Å and 1.9 Å; O-Tyr329; 1.9 Å). (b) Superimposition of compound F1b and BIQ in PHD2.Fe(II) in the comparably narrow slot-shaped active site pocket. 48
- Figure 3.4 (a) The docked conformation of compound F1c in PHD2.Fe(II) complex. Compound F1c chelates the ferrous ion (cyan) through its benzothiazole ring sulphur atom (yellow) (S-Fe[II]; 3.1 Å) and carbonyl oxygen (red) (O-Fe[II]; 1.5 Å). The formation of hydrogen bond through the carboxylate oxygen and active site protein residue (magenta) (O-Arg383; 2.3 Å and 2.1 Å; O-Tyr329; 1.7 Å). (b) Superimposition of compound F1c and BIQ in PHD2.Fe(II) in the comparably narrow slot-shaped active site pocket. 49
- Figure 3.5 (a) The docked conformation of compound F1d in PHD2.Fe(II) complex. Compound F1d chelates the ferrous ion (cyan) through its benzothiazole ring nitrogen atom (blue) (N-Fe[II]; 1.8 Å). The formation of hydrogen bond through the nitro group oxygen and active site protein residue (magenta) (O-Arg383; 1.8 Å, 1.8 Å and 2.2 Å; O-Tyr329; 1.7 Å and 2.4 Å). (b) Superimposition of compound F1d and BIQ in PHD2.Fe(II) in the comparably narrow slot-shaped active site pocket. 50
- Figure 3.6 (a) The docked conformation of compound F2a in PHD2.Fe(II) complex. Compound F2a chelates the ferrous ion (cyan) through its benzoxazole ring oxygen (red) (O-Fe[II]; 2.1 Å), amide nitrogen (N-Fe[II]; 2.9 Å), carbonyl oxygen (O-Fe[II]; 1.5 Å). The formation of hydrogen bond through the carboxylate oxygen and active site protein residue (magenta) (O-Arg383; 1.9 Å and 1.9 Å; O-Tyr329; 51

1.8 Å). (b) Superimposition of compound F2a and BIQ in PHD2.Fe(II) in the comparably narrow slot-shaped active site pocket.

- Figure 3.7 (a) The docked conformation of compound F2B in PHD2.Fe(II) complex. Compound F2b chelates the ferrous ion (cyan) through its benzoxazole ring oxygen (red) (O-Fe[II]; 2.1 Å) and carbonyl oxygen (O-Fe[II]; 1.5 Å). The formation of hydrogen bond through the carboxylate oxygen and active site protein residue (magenta) (O-Arg383; 1.9 Å and 1.9 Å; O-Tyr329; 1.8 Å). (b) Superimposition of compound F2b and BIQ in PHD2.Fe(II) in the comparably narrow slot-shaped active site pocket. 52
- Figure 3.8 (a) The docked conformation of compound F3a in PHD2.Fe(II) complex. Compound F3a chelates the ferrous ion (cyan) through its imidazole ring nitrogen (blue) (N-Fe[II]; 2.2 Å) and carbonyl oxygen (O-Fe[II]; 1.5 Å). The formation of hydrogen bond through the carboxylate oxygen and active site protein residue (magenta) (O-Arg383; 1.7 Å and 1.9 Å; O-Tyr329; 1.9 Å). (b) Superimposition of compound F3a and BIQ in PHD2.Fe(II) in the comparably narrow slot-shaped active site pocket. 53
- Figure 3.9 (a) The docked conformation of compound F4a in PHD2.Fe(II) complex. Compound F4a chelate the ferrous ion (cyan) through its isoquinoline ring nitrogen (blue) (N-Fe[II]; 2.5 Å) and carbonyl oxygen (O-Fe[II]; 1.5 Å). The formation of hydrogen bond through the carboxylate oxygen and active site protein residue (magenta) (O-Arg383; 2.1 Å and 1.8 Å; O-Tyr329; 1.8 Å). (b) Superimposition of compound F4a and BIQ in PHD2.Fe(II) in the comparably narrow slot-shaped active site pocket. 54
- Figure 3.10 (a) The docked conformation of compound F3a in PHD2.Fe(II) complex. Compound F5a chelate the ferrous ion (cyan) through its thiazole ring nitrogen (blue) (N-Fe[II]; 2.5 Å) and carbonyl oxygen (O-Fe[II]; 1.5 Å). The formation of hydrogen bond through the carboxylate oxygen and active site protein residue (magenta) (O-Arg383; 2.1 Å and 1.9 Å; O-Tyr329; 1.8 Å). (b) Superimposition of compound F5a and BIQ in PHD.Fe(II) in the comparably narrow slot-shaped active site pocket. 55
- Figure 3.11 (a) The docked conformation of compound F5b in PHD2.Fe(II) complex. Compound F5b chelates the ferrous ion (cyan) through its thiazole ring nitrogen (blue) (N-Fe[II]; 3.3 Å) and carbonyl oxygen (O-Fe[II]; 1.5 Å). The 56

formation of hydrogen bond through the carboxylate oxygen and active site protein residue (magenta) (O-Arg383; 1.7 Å and 1.9 Å; O-Tyr329; 1.8 Å). (b) Superimposition of compound F5b and BIQ in PHD2.Fe(II) in the comparably narrow slot-shaped active site pocket.

- Figure 3.12 (a) The docked conformation of compound F6a in PHD2.Fe(II) complex. Compound F6a chelates the ferrous ion (cyan) through its thiazole ring nitrogen (blue) (N-Fe[II]; 2.8 Å) and carbonyl oxygen (O-Fe[II]; 1.5 Å). The formation of hydrogen bond through the carboxylate oxygen and active site protein residue (magenta) (O-Arg383; 1.7 Å and 1.9 Å; O-Tyr329; 2.0 Å). (b) Superimposition of compound F6a and BIQ in PHD2.Fe(II) in the comparably narrow slot-shaped active site pocket. 57
- Figure 3.13 (a) The docked conformation of compound F7a in PHD2.Fe(II) complex. Compound F7a chelates the ferrous ion (cyan) through its pyrazole ring nitrogen (blue) (N-Fe[II]; 2.4 Å) and carbonyl oxygen (O-Fe[II]; 1.6 Å). The formation of hydrogen bond through the carboxylate oxygen and active site protein residue (magenta) (O-Arg383; 1.7 Å and 1.9 Å; O-Tyr329; 1.9 Å). (b) Superimposition of compound F7a and BIQ in PHD2.Fe(II) in the comparably narrow slot-shaped active site pocket. 58
- Figure 3.14 (a) The docked conformation of compound F8a in PHD2.Fe(II) complex. Compound F8a chelates the ferrous ion (cyan) through its amide nitrogen (blue) and oxygen (red) (N-Fe[II]; 3.1 Å; O-Fe[II]; 1.5 Å). The formation of hydrogen bond through the carboxylate oxygen and active site protein residue (magenta) (O-Arg383; 1.8 Å and 1.8 Å; O-Tyr329; 1.9 Å). (b) Superimposition of compound F8a and BIQ in PHD2.Fe(II) in the comparably narrow slot-shaped active site pocket. 59
- Figure 3.15 (a) The docked conformation of compound F9a in PHD2.Fe(II) complex. Compound F9a chelates the ferrous ion (cyan) through its sulfonyl and carbonyl oxygen (red) (SO-Fe[II]; 1.6 Å; O-Fe[II]; 1.7 Å). The formation of hydrogen bond through the carboxylate oxygen and active site protein residue (magenta) (O-Arg383; 2.0 Å and 1.9 Å; O-Tyr329; 1.8 Å). (b) Superimposition of compound F9a and BIQ in PHD.Fe(II) in the comparably narrow slot-shaped active site pocket. 60
- Figure 3.16 (a) The docked conformation of compound F9a in PHD2.Fe(II) complex. Compound F9b chelates the ferrous 61

ion (cyan) through its sulfonyl oxygens (red) (SO-Fe[III]; 1.4 Å; SO-Fe[II]; 3.1 Å). The formation of hydrogen bond through the carboxylate oxygen and active site protein residue (magenta) (O-Arg383; 1.8 Å and 1.9 Å; O-Tyr329; 1.8 Å). (b) Superimposition of compound F9b and BIQ in PHD2.Fe(II) in the comparably narrow slot-shaped active site pocket.

Figure 3.17	The proposed mechanism of the nucleophilic addition of amine to succinic anhydride to form 4-oxobutanoic acid analogues.	64
Figure 3.18	The proposed mechanism of nucleophilic addition reaction of sulfonamides with succinic anhydride to form 4-oxobitanoic acid analogue.	66
Figure 3.19	¹ H NMR Spectrum of F1a	76
Figure 3.20	¹³ C NMR Spectrum of F1a	77
Figure 3.21	¹ H – ¹ H COSY Spectrum of F1a	78
Figure 3.22	HSQC Spectrum of F1a	79
Figure 3.23	HMBC Spectrum of F1a	80
Figure 3.24	Selected COSY and HMBC correlation of F1a	81
Figure 3.25	FT-IR Spectrum of F1a	82
Figure 3.26	-ESI DIMS Spectrum of F1a	83
Figure 3.27	¹ H NMR Spectrum of F1b	86
Figure 3.28	¹³ C NMR Spectrum of F1b	87
Figure 3.29	¹ H NMR Spectrum of F1c	90
Figure 3.30	¹³ C NMR Spectrum of F1c	91
Figure 3.31	¹ H NMR Spectrum of F1d	94
Figure 3.32	¹³ C NMR Spectrum of F1d	95
Figure 3.33	¹ H NMR Spectrum of F2a	98
Figure 3.34	¹³ C NMR Spectrum of F2a	99

Figure 3.35	¹ H NMR Spectrum of F2b	102
Figure 3.36	¹³ C NMR Spectrum of F2b	103
Figure 3.37	¹ H NMR Spectrum of F3a	106
Figure 3.38	¹³ C NMR Spectrum of F3a	107
Figure 3.39	¹ H NMR Spectrum of F4a	110
Figure 3.40	¹³ C NMR Spectrum of F4a	111
Figure 3.41	¹ H NMR Spectrum of F5a	114
Figure 3.42	¹³ C NMR Spectrum of F5a	115
Figure 3.43	¹ H NMR Spectrum of F5b	118
Figure 3.44	¹³ C NMR Spectrum of F5b	119
Figure 3.45	¹ H NMR Spectrum of F6a	122
Figure 3.46	¹³ C NMR Spectrum of F6a	123
Figure 3.47	¹ H NMR Spectrum of F7a	126
Figure 3.48	¹³ C NMR Spectrum of F7a	127
Figure 3.49	¹ H NMR Spectrum of F8a	130
Figure 3.50	¹³ C NMR Spectrum of F8a	131
Figure 3.51	¹ H NMR Spectrum of F9a	134
Figure 3.52	¹³ C NMR Spectrum of F9a	135
Figure 3.53	¹ H NMR Spectrum of F9b	138
Figure 3.54	¹³ C NMR Spectrum of F9b	139
Figure 3.55	The half-maximal inhibitory concentration (IC ₅₀) of (a) F2a (b) F2b (c) F3a (d) FG-4592 against PHD-2.	143

LIST OF SCHEMES

	Page	
Scheme 1.1	Reaction of cyclic anhydrides with aromatic primary amines.	17
Scheme 1.2	Reaction of cyclic and acyclic anhydrides with amine in aqueous medium	18
Scheme 3.1	The general synthesis procedure of 4-oxobutanoic acid analogues using primary amine and succinic anhydride	62
Scheme 3.2	The general synthesis procedure of 4-oxobutanoic acid analogues using sulfonamides and succinic anhydride	65

LIST OF ABBREVIATIONS

2-OG	2-Oxoglutarate
2,4-PDCA	2,4-Pyridinedicarboxylate
4HQs	4-Hydroxy-2-oxo-1,2-dihydroquinoline derivative
DPCA	4-Oxo-1,4-dihydro-1,10-phenanthroline-3-carboxylic acid glycinamide analogue
^{13}C NMR	Carbon Nuclear Magnetic Resonance
^1H - ^1H COSY	Correlation Spectroscopy
DCM	Dichloromethane
DMF	Dimethylformamide
DMSO	Dimethyl sulfoxide
DI-MS	Direct Infusion Mass Spectrometry
EPO	Erythropoietin
FIH	Factor inhibiting HIF
FTIR	Fourier Transform Infrared Spectroscopy
HREs	Hypoxia response elements
HMBC	Heteronuclear Multiple Quantum Coherence
HSQC	Heteronuclear Single Quantum Coherence
NODD	<i>N</i> -Terminal oxygen dependent degradation domain

Pro564	Proline residue 564
$^1\text{H NMR}$	Proton Nuclear Magnetic Resonance
VEGF	Vascular endothelial growth factor
δ	Chemical Shift
J	Coupling Constant
$^{\circ}\text{C}$	Degree Celcius
d	Doublet
dd	Doublet of Doublet
IC_{50}	Half-maximal inhibitory concentration
Kg	Kilogram
m/z	Mass per Charge
MHz	Mega Hertz
m	Meter
μM	Micromolar
m	Multiplet
nM	Nanomolar
ppm	Part per Million
s	Singlet
t	Triplet

**REKA CIPTA, SINTESIS DAN PENCIRIAN ANALOG ASID 4-
OKSOBUTANOIK YANG BERPOTENSI SEBAGAI PERENCAT FAKTOR
PENDORONG HIPOKSIA MANUSIA (HIF) PROLIL HIDROKSILASI 2 (PHD-
2)**

ABSTRAK

Terdapat penyedaran minat dalam mengembang perencat faktor pendorong hipoksia manusia (HIF) prolil hidroksilasi bagi merawat penyakit iskemik/hipoksik. Dalam kajian ini, satu siri baru analog asid 4-Oksobutanoik yang berpotensi telah diselidik sebagai perencat HIF prolil hidroksilasi 2 (PHD-2). Sebatian tersebut direka berdasarkan kebolehan perencat mengikat secara bidentat pada tapak aktif PHD-2, dari segi bentuk pengikatan yang paling sesuai dengan menggunakan *Autodock 4.0* dan *Accelrys Discovery Studio 4.0*. Analog asid 4-Oksobutanoik telah disintesis menggunakan amina dan sulfonamida bersama suksinik anhidrida. Sebatian yang telah disintesis lalu dicirikan menggunakan 1D-NMR (^1H , ^{13}C), 2D-NMR (COSY, HSQC dan HMBC), FTIR, analisis unsur CHN dan DIMS. Sistem cerakin RapidFire PHD-2 digunakan sebagai kajian lanjutan untuk mengenal pasti potensi perencatan analog asid 4-Oksobutanoik terhadap PHD-2. Hasil cerakin RapidFire PHD-2 *in vitro* menunjukkan bahawa sebatian **F2a** dan **F2b** ialah perencat berpotensi, dengan nilai IC_{50} masing-masing 242 nM dan 160 nM, diikuti dengan **F3a** dengan nilai IC_{50} 71.2 μM . F2a dan F2b didapati lebih berpotensi dalam merencatkan PHD-2 daripada calon kawalan positif FibroGen FG4592 yang kini sedang menjalani fasa ketiga klinikal dalam merawat anemia pada pesakit yang mempunyai penyakit ginjal kronik (CKD).

**DESIGN, SYNTHESIS AND CHARACTERIZATION OF 4-OXOBUTANOIC
ACID ANALOGUES AS POTENTIAL HUMAN HYPOXIA INDUCIBLE
FACTOR (HIF) PROLYL HYDROXYLASE DOMAIN 2 (PHD-2) INHIBITORS**

ABSTRACT

There is a widespread interest in developing the human hypoxia inducible factor (HIF) prolyl hydroxylase inhibitors for the treatment of ischemic/hypoxic diseases. In this study, a new series of 4-oxobutanoic acid analogues was investigated as potential HIF prolyl hydroxylase domain-2 (PHD-2) inhibitors. The compounds were designed based on their binding capabilities to the PHD-2 active sites in a bidentate manner, with the most favorable binding modes in the molecular docking studies using Autodock 4.0 and Accelrys Discovery Studio 4.0. The compounds were synthesized by reacting amines and sulfonamides with succinic anhydride. The synthesized compounds were further characterized using 1D-NMR (^1H , ^{13}C), 2D-NMR (COSY, HSQC and HMBC), FTIR, CHN elemental analysis and DIMS. PHD-2 RapidFire assay was further employed to determine the *in vitro* inhibitory potencies of the 4-oxobutanoic acid analogues against PHD-2. The assay results revealed that compounds **F2a** and **F2b** were potent PHD-2 inhibitors, with IC_{50} values of 242 nM and 160 nM, respectively followed by **F3a** with IC_{50} value of 71.2 μM . F2a and F2b were found to be more potent in inhibiting PHD-2 than the positive control in the assay, FibroGen's candidate FG-4592 which is undergoing clinical third phase in treating anemia in patient with chronic kidney disease (CKD).

CHAPTER 1

INTRODUCTION AND LITERATURE REVIEW

1.1 Hypoxia

Hypoxia is defined as the failure of oxygenation at the tissue level (Samuel & Franklin, 2008). Oxygen homeostasis is a fundamental yet crucial process for all organisms to survive. Upon the commencement of hypoxic conditions, cells and tissues trigger several adaptive responses to stabilize the energy consumption by increasing the ventilation, cardiac output, vascularization, oxygen transport capacity in haemoglobin as well as switching mode of metabolism, from aerobic into anaerobic. Prolong exposure to low oxygen conditions lead to the mediation of up-regulated genes encoding key actor for dopamine synthesis, anaerobic glycolysis, angiogenesis elicitation, erythrocyte proliferation and neuro protection. These responses are all mediated by the action of hypoxia inducible factor (HIF) (Hirota *et al.*, 2006; Semenza, 2000).

1.2 Hypoxia Inducible Factor (HIF)

In the early 90s, an important finding from Semenza who purified hypoxia inducible factor (HIF) and subsequently continued with Wang (1992) using a DNA affinity column comprised of the *cis*-acting element (5'[A/G]CGTG-3'), generally known as hypoxia response element (HRE) proved the important role of HIF in regulating transcriptional activity in response to short- and long term adaptation of

oxygen needing conditions which is detrimental to mammalian cells. Hence, HIF was indubitably given the appellation “master of regulator”.

HIF is a heterodimeric transcription factor that comprises of a constitutively expressed oxygen resistant β -subunit (HIF- β) and hypoxia regulated oxygen-labile α -subunit (HIF-1 α , HIF-2 α and HIF-3 α) (Ema et al., 1997; Flamme et al., 1997; Tian et al., 1997). Both subunits pertaining to basic helix-loops-helix (bHLH), PER-ARNT-SIM (PAS) superfamily of transcription factors. The bHLH consist of two highly distinguishing and conserved domain, basic (b) and HLH region. The basic region play a role in the binding of transcription factor to DNA while HLH region aid protein-protein interactions. The PAS domains (PAS A and PAS B) that consist of 200-350 amino acids stretch showed a high sequence homology to protein domains (Savouret *et al.*, 2001).

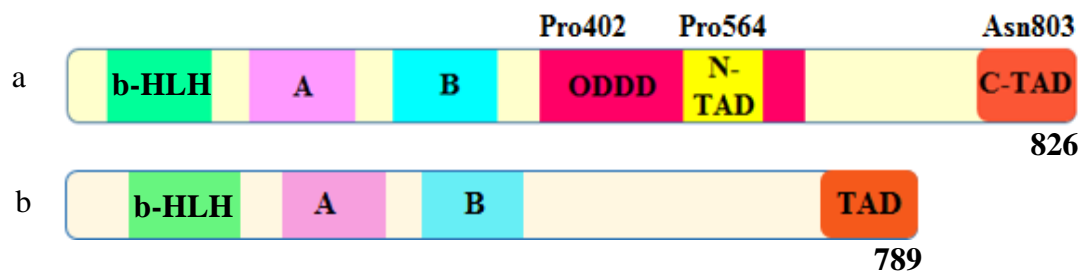


Figure 1.1: Schematic sketching of HIF isoform: (a) HIF-1 α . (b) HIF-1 β . Abbreviations for N-TADN and C-TAD: Amino-terminal and carboxy-terminal transactivating domains; b-HLH: Basic helix loop-helix for DNA binding; PAS A and Pas B: Protein domain critical for dimerization. At the end of structure, the total number of amino acids for each subunit was labelled. (Figure reviewed from Hellwig-Bürigel, 2009; Ke and Costa, 2006; Semenza *et al.*, 1998)

Among the isoforms, HIF-1 was studied most comprehensively and close up to scrutiny. The HIF-1 α and HIF-1 β subunits are shown in Figure 1.1. In mRNA levels, both HIF-1 α and HIF-1 β , expressed constantly regardless of the partial pressure of oxygen due to the presence of an internal ribosome entry site (IRES) in their corresponding mRNA which consequently leads to the cap-independent translation of HIF pattern (Hellwig-Bürigel, 2009; Lang *et al.*, 2002). However, HIF-1 α is fully

dependent on the oxygen tension but not HIF-1 β especially in protein levels. Despite oxygen level depreciates below the normal range, HIF-1 β subunit expression is not affected by the fluctuation of cellular oxygen levels and yet still able to express at constant level. HIF-1 α is the most ubiquitously expressed α subunit in metazoans and have more expression patterns compared to HIF-2 α and HIF-3 α .

1.3 Hypoxia Signaling Pathway

HIF-1 activation begin with the stabilization and storing up of HIF-1 α . Appropriate redox conditions and post-translational modifications such as hydroxylation, ubiquitination, acetylation and phosphorylation contributed to the completion of full transcriptional activity (Brahimi-Horn *et al.*, 2002; Huang and Bunn, 2003; Minet *et al.*, 2001). HIF does not respond directly to the cellular oxygen levels as mentioned by Yan *et al.*, (2010). Instead, HIF prolyl hydroxylase domain (PHD) enzymes played the role and catalyze the HIF prolyl hydroxylation. There are three isoforms of PHD enzymes, namely prolyl hydroxylase-1 (PHD-1), prolyl hydroxylase-2 (PHD-2) and prolyl Hydroxylase-3 (PHD-3). On the other hand, factor inhibiting HIF (FIH) is a negative regulator of HIF- α , catalyzed the HIF asparaginyl hydroxylation. Both PHDs and FIH are 2-OG/Fe²⁺ dependent dioxygenases which utilize oxygen as co-substrate for catalysis purpose as shown in Figure 1.2.

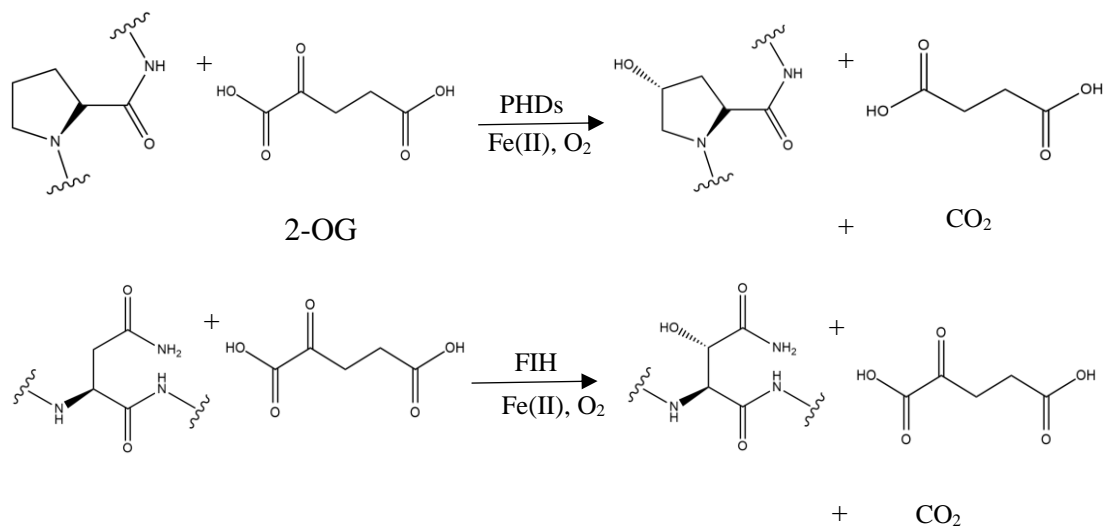


Figure 1.2: HIF prolyl hydroxylases (PHDs) and Factor inhibiting HIF (FIH) utilizing ferrous ion (Fe²⁺), 2-oxoglutarate (2-OG) and oxygen (O₂) as cofactor/co-substrate to catalyze hydroxylation, forming hydroxy-proline/asparagine residue, succinate and carbon dioxide (Epstein *et al.*, 2001; McDonough *et al.*, 2006).

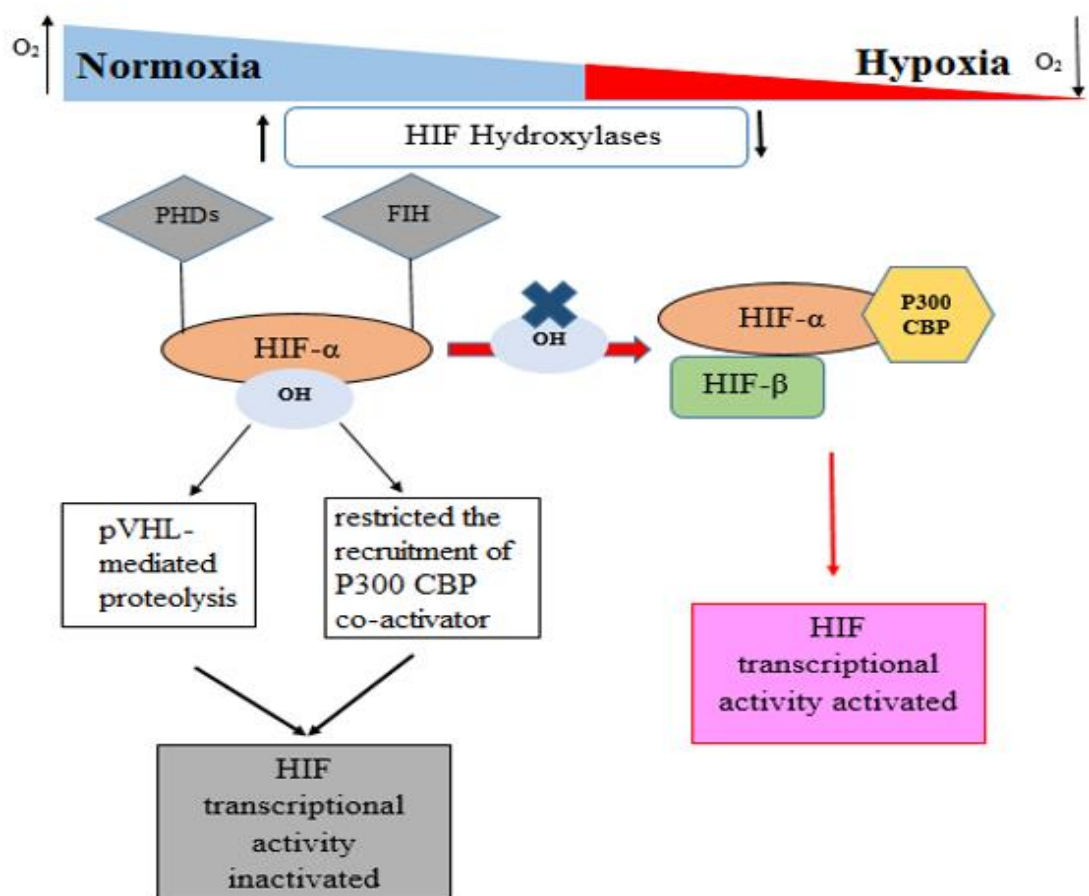


Figure 1.3: The HIF transcriptional pathway: oxygen sensing and signaling under normoxic and hypoxic conditions by PHDs and FIH. Figure reviewed from Yan *et al.*, 2010.

Figure 1.3 illustrates the HIF transcriptional pathway under hypoxic and normoxic conditions by PHD and FIH. PHDs and FIH are extremely important in mediated the hypoxia signaling pathway. Under normoxic condition, two conserved proline residues in HIF-1 α undergoes prolyl hydroxylation within the oxygen-degradation domain (ODD): Pro402 in the *N*-terminal oxygen-dependent degradation domain (NODD) and Pro564 in the *C*-terminal oxygen dependent degradation domain (CODD), catalyzed by the PHDs in the presence of ferrous ion (Fe²⁺) and 2-oxoglutarate (2-OG). This in turn recruits the tumor suppressor protein von Hippel-Lindau (pVHL), a substrate-recognition subunit of an E3 ubiquitin ligase complex to bind and activate the proteolysis of HIF-1 α . The average half-life of HIF-1 α is extremely short (< 5 minute) and rapidly degraded through ubiquitin-proteasome pathway (Huang *et al.*, 1996). At the same time, β -hydroxylation of conserved asparagine residue (Asn803) by FIH within the *C*-terminal transcriptional activation domain (C-TAD) restrains the uptake of co-activator proteins p300/CBP, rendering the inactivation of HIF transcriptional activity (Hirota and Semenza, 2005).

However, when cellular oxygen consumption surpasses oxygen supply, PHD-activity is significantly reduced and the hydroxylation of HIF-1 α subunits is restricted. This in turn results in the stabilization and accumulation of HIF-1 α . This is in accordance to the statement from Huang *et al.*, (1998) that HIF-1 α is only detectable under hypoxic condition. Hypoxic conditions elevate the half-life of HIF-1 α and subsequently translocated it into nucleus in order to dimerize with HIF-1 β to form functionally heterodimers HIF-1 (HIF1 α /HIF1 β). HIF-1 binds to HREs to induce the gene transcription. At the same time, the co-activator complex p300/CBP being recruited and binds to the C-TAD region which promote the transcription of hypoxia-inducible genes. (Cockman *et al.*, 2000; Semenza *et al.*, 1996; Yan *et al.*, 2010).

1.4 Prolyl Hydroxylase Domain (PHDs)

Three independent genes have been identified coded on the human PHDs, namely PHD-1, PHD-2 and PHD-3. Human PHDs consist of two structural domains: highly conserved catalytic C-terminal, and N-terminal which is more divergent with limited characterization. PHDs are soluble proteins and possess about 55% similarity at the catalytic C-terminal (Epstein *et al.*, 2001). PHDs are well known as an effective oxygen sensor due to their characteristics: first, its high K_m values ($\approx 240 \mu\text{M}$) which are slightly higher than the atmospheric dissolved oxygen ($\approx 200 \mu\text{M}$) and second, their slow reaction rates with oxygen. The high K_m values of the PHDs providing a sensitive assay to detect the fluctuation of oxygen tensions (Ehrishman *et al.*, 2007; Hirsilä *et al.*, 2003).

PHD-1 is predominantly found in nucleus with 409 amino acid residues (Metzen *et al.*, 2003). It is highly expressed in testis followed by liver, heart, brain and kidney. However, a PHD-1 knockout study shows that the shortage of PHD-1 did not bring much influence on male fertility. Instead, PHD-2 which is recognized as the most abundant isoform, may have functions overlap with PHD-1 in playing the role in maintaining the reproductive capability in testis (Lieb *et al.*, 2002). According to Cioffi *et al.*, (2003), PHD-1 is induced by estrogen for cell proliferation due its nature of non-responsive to hypoxia in mRNA levels.

PHD-2 is primarily present in cytoplasm, and sometimes in the nucleus. (Metzen *et al.*, 2003; Soilleux *et al.*, 2005; Steinhoff *et al.*, 2009). It is also the longest isoform among the human PHDs with 426 amino acids residues, found most abundance in heart and testis (Lieb *et al.*, 2002). PHD-2 is specifically induced by HIF-1 α and it is crucial in sensing oxygen levels in the HIF degradation pathway. Appelhoff *et al.*, (2004) reported that the reduction in PHD-2 increases the levels of HIF-1 α under normoxic

conditions. A human PHD-2 allele mutational study by Percy *et al.*, (2006) shows that reduction of PHD-2 activity is able to increase erythropoietin (EPO) production. In the following years, Takade and colleagues (2007) carried out a PHD-2/PHD-3 mutation study in liver, found that PHD-2 is significantly bias to the stabilization of HIF-1 α instead of HIF-2 α , while PHD-3 is vice versa. The study also reported that PHD-2 is the key isoform in adult vascular system.

PHD-3 was found in both nucleus and cytoplasm with 239 amino acid residues, and highly predominates in heart (Metzen *et al.*, 2003). PHD-3 possess significant impact on HIF system. It has been reported that PHD-3 is able to prolong the half-life of HIF- α subunits during re-oxygenation and keeping induction for a continuous hypoxic conditions (Appelhoff, *et al.*, 2004). In addition, PHD-3 assures the elimination of excessive HIF- α after re-oxygenation (Fong and Takeda, 2008). Figure 1.4(a) shows the sequence alignment of PHD1-3.

Up to this date, PHD-2 is the only isoform that it's structure has been solved in crystallographic studies among PHDs. Figure 1.4 (b) shows the crystal structure of PHD-2 in complex with 8-iodo bicyclic isoquinoline, revealing it is made up of eight major antiparallel β -strands (also known as double stranded β helix, DSBH), three conserved α -helices (α -1, α -2, α -3) and other minor β -sheets pack along the DSBH core. Another C-terminal α -helix (α -4) stretches from the β -10. On top of that, cofactor ferrous ion (Fe^{2+}) was buried deeply in the active site pocket, coordinated by a set of ligands (His313, Asp315, His374) in tridentate manner forming the $\text{Fe}^{2+}/2\text{-OG}$ complexes (McDonough *et al.*, 2006). Upon binding of PHD-2 to the HIF-1 α , the hydroxylation site and the complexes are separated due to the CODD HIF-1 α structural changes (Chowdhury *et al.*, 2009).

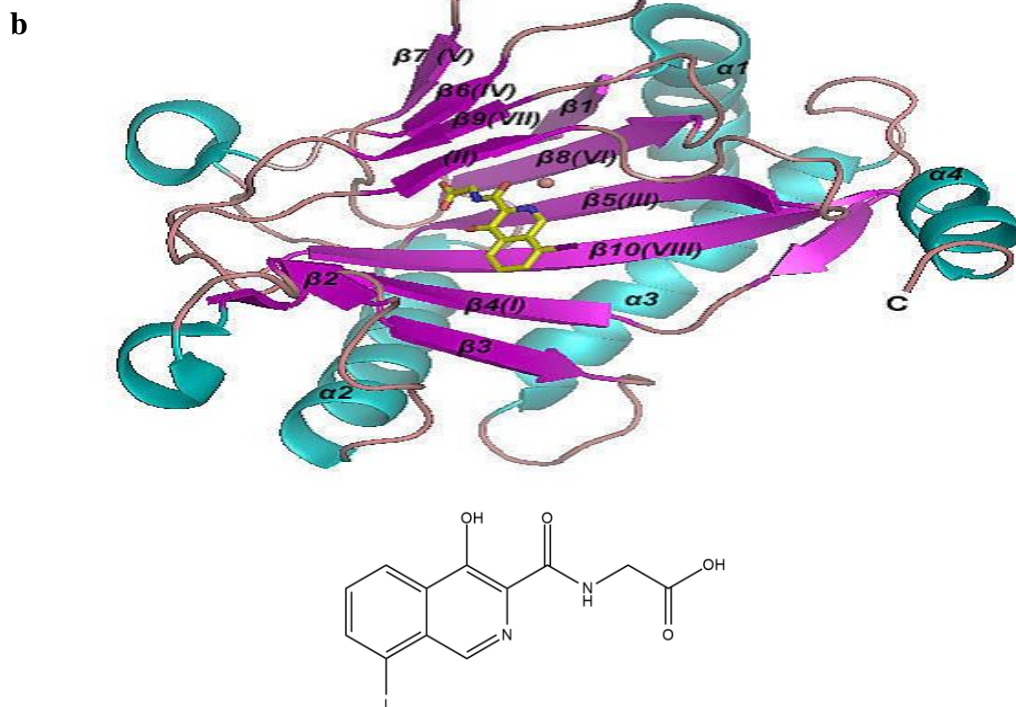
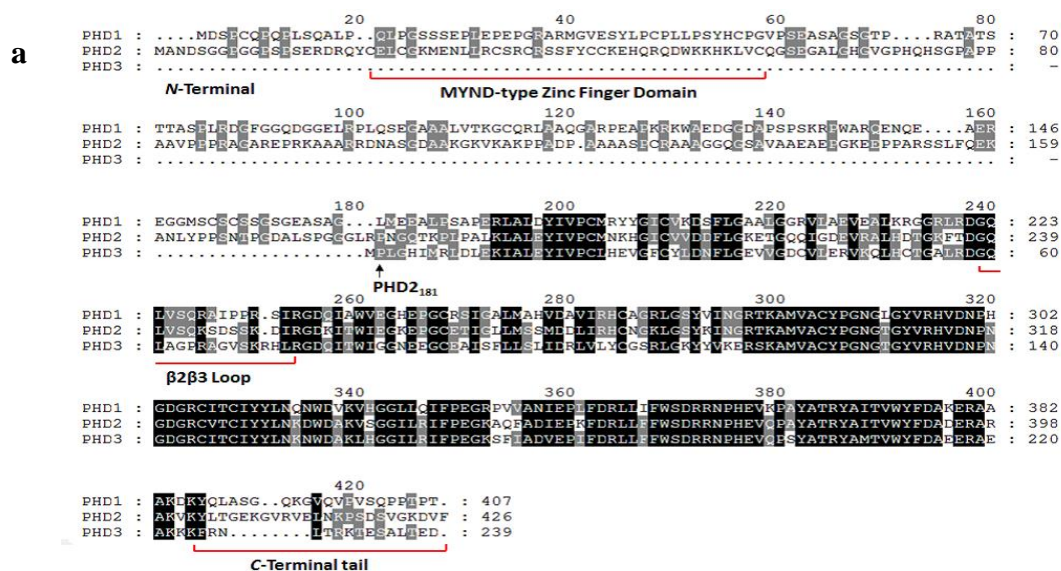


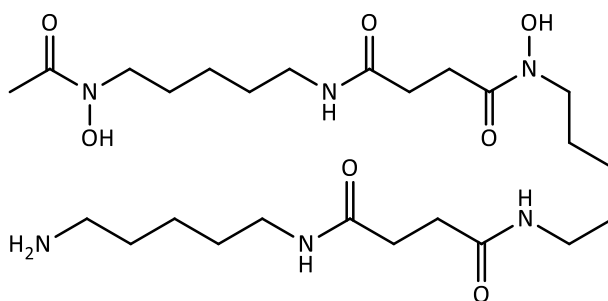
Figure 1.4: (a) Sequence alignment of Human PHD-1, PHD-2 and PHD-3. Residues shaded with black were highly conserved sequence similarities (Flashman *et al.*, 2008). (b) Ribbon presentation of crystallographic PHD-2 (cyan and violet) in complex with 8-iodo bicyclic isoquinoline (yellow) and iron (pink). The eight major β -strands of DSBH are highlighted in violet and numbered (β I- β VIII) and α -helices in cyan (α 1- α 4). (Figure adapted from the Protein Data Bank www.pdb.com)

1.5 PHD Inhibitors

Different classes of prolyl hydroxylase domains 2 (PHD-2) inhibitors have been developed and reported in recent years, arises from their isoforms abundance and crucial role in regulating HIF- α subunits.

1.5.1 Iron chelator

The iron chelator desferrioxamine (DFO) is the first reference compound in PHD inhibition related studies, for its role in elevating erythropoietin RNA and HIF-1 α levels in cells. DFO is a non-competitive inhibitor which chelates and occupies iron (Fe^{2+}) in the active site and subsequently deactivate the HIF prolyl hydroxylases. However, based on the finding of Hirsilä *et al.* (2005), DFO did not inhibited crude type PHD-2 at all up to 1mM concentration but inhibited about 40-50% of the activity of purified PHD-2 at 10 μM .



Desferrioxamine (DFO)

1.5.2 Divalent transition metal ions

PHDs are inhibited through the competition of divalent transition metal ions such as Co^{2+} , Cu^{2+} , Zn^{2+} , Mn^{2+} , Ni^{2+} or Cd^{2+} with respect to Fe^{2+} . Among the divalent metal ions, Cu^{2+} shows the most potent inhibitory activity followed by Zn^{2+} , Mn^{2+} , Co^{2+} , Cd^{2+} and lastly Ni^{2+} (Sekirnik *et al.*, 2005). The IC_{50} values of these transition metal ions against PHD-2 are summarized in Table 1.1.

Table 1.1: The IC₅₀ values of various divalent transition metal ions against PHD-2 (Sekirnik *et al.*, 2005).

	IC ₅₀ (μM)					
	Zn ²⁺	Mn ²⁺	Co ²⁺	Ni ²⁺	Cu ²⁺	Cd ²⁺
PHD-2	9.3	21	48.3	185.2	6.6	57.4

1.5.3 2-OG competitive PHD inhibitors

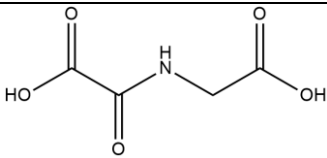
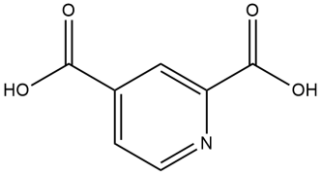
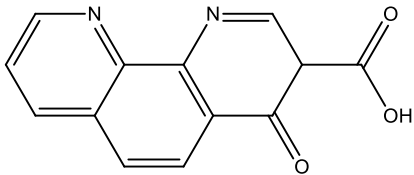
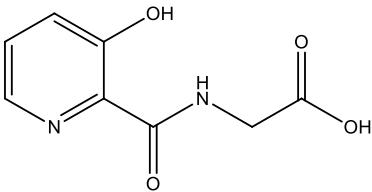
On top of that, 2-OG competition is another mechanism use to inhibit PHDs. Most of the reported inhibitors compete with 2-OG or probably oxygen and chelate to the active site metal ion in bidentate fashion. In 1995, Baader *et al.*, found that *N*-oxalyglycine (NOG) is a potent PHD inhibitor and its binding mode is through 2-OG competition. The carboxylate and amide oxygen of NOG chelate to the manganese ion (Mn²⁺), substituting ferrous ion (Fe²⁺) in bidentate manner (Epstein *et al.*, 2001) in the PHD2-NOG complex crystallographic study.

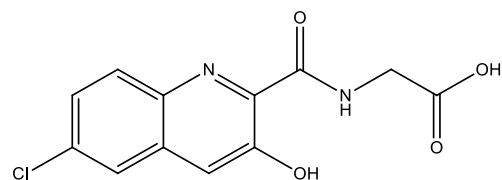
Others reported 2-OG mimic inhibitors such as 2,4-pyridinedicarboxylate (2,4-PDCA), 3-hydroxypyridine-2-carbonyl-glycine, 2-(3-hydroxypicolinamido)acetic acid and *N*-((3-hydroxy-6-chloroquinolin-2-yl)carbonyl)glycine showed satisfactory inhibitory activity against PHD-2 (Table 1.2). However, NOG and 2,4-PDCA have been reported as non-selective PHDs inhibitor as these simple 2-OG mimic inhibitors also inhibited wide range of 2-OG oxygenases (Chowdhury *et al.*, 2013).

In 2003, FibroGen, InC. reported that 1-chloro-4-hydroxyisoquinoline glycinamide or bicyclic isoquinoline (BIQ) as a PHD-2 inhibitor and declared it as their first clinical candidate in 2008, named as FG-2216 and FG-4592 as backup candidate (Thevis *et al.*, 2008). Another derivative compound of BIQ: L-Ala BIQ showed less potent inhibitory activity as compared to BIQ. Furthermore, a series of 4-hydroxy-2-oxo-1,2-dihydroquinoline derivative (4HQs) were reported as selective PHD-2 inhibitors which is 4HQs-4, 4HQs-6 and 4HQs-9 (Chowdhury *et al.*, 2013).

On top of that, Barrett *et al.*, 2011 characterized a pharmacological compound 1-(5-chloro-6-(trifluoromethoxy)-1*H*-benzoimidazol-2-yl)-1*H*-pyrazole-4-carboxylic acid (JNJ-42041935) as potent and selective PHD-2 inhibitor. Deng *et al.*, (2013) also discovered 2,8-Diazaspiro [4.5] decan-1-ones as potent, orally bioavailable PHD2 inhibitors. The reported IC₅₀ value for the PHD-2 inhibitors are summarized in Table 1.2. The discrepancies in the reported IC₅₀ values reflected the variations especially assay conditions in the respective experiments.

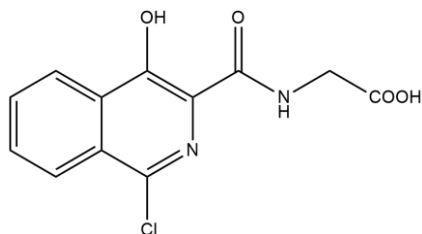
Table 1.2: The reported IC₅₀ values of 2-OG competitive inhibitors against PHD-2

Inhibitor	IC ₅₀ (μM)
	PHD-2
 <p>NOG</p>	8 ^a , 0.8 ^c
 <p>2,4-PDCA</p>	7 ^a , 6 ^b
 <p>DPCA</p>	10 ^a
 <p>3-Hydroxypyridine-2-carbonyl-glycine</p>	2 ^a



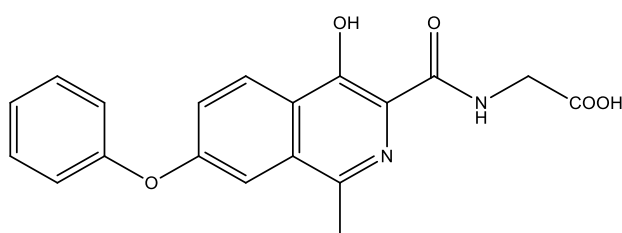
0.2^a

N-((3-hydroxy-6-chloroquinolin-2-yl)carbonyl)glycine



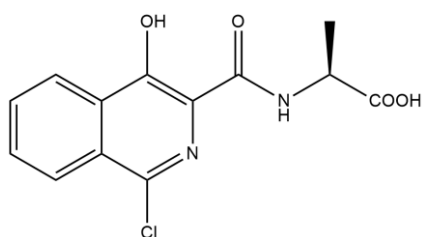
0.3^d, 1.4^e, 3.9^f

BIQ / FG-2216



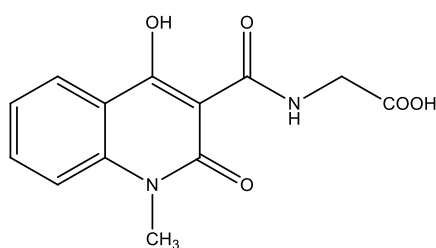
0.59^g

FG-4592



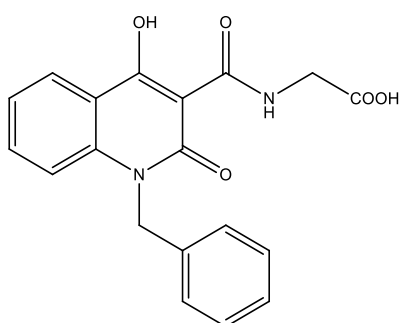
1.1^e

L-Ala BIQ



0.033^e

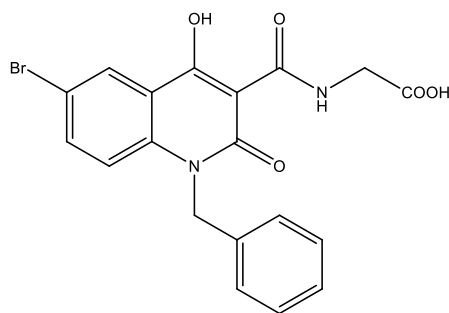
4HQs-4



0.022^e

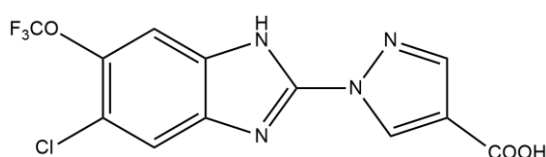
4HQs-6

0.078^e



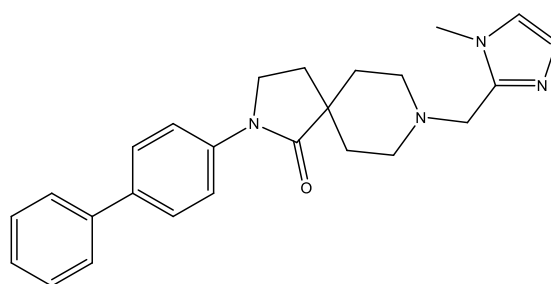
4HQs-9

7.00±0.05μM^g



JNJ-42041935

1.3^h



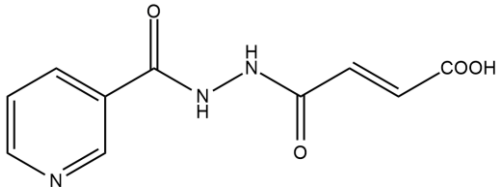
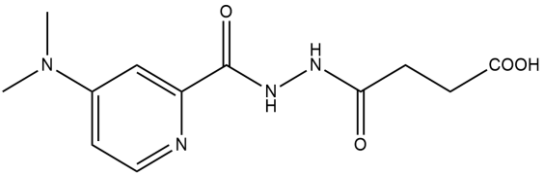
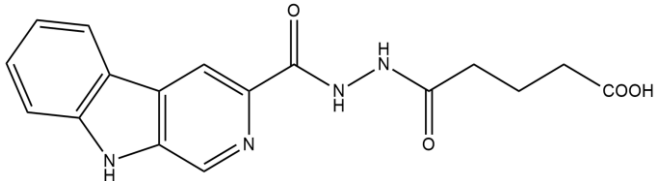
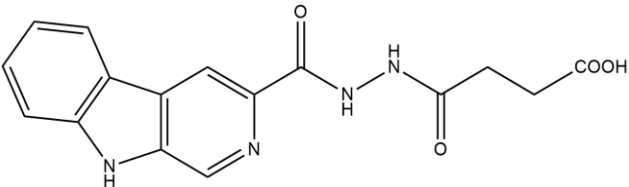
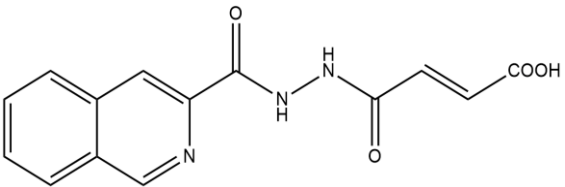
2, 8-Diazaspiro [4.5] decan-1-ones

The IC₅₀ value^a, value^b, value^c, value^d, value^e, value^f, value^g, value^h and valueⁱ were reported by Hirsilä *et al.*, (2005); King *et al.*, (2010); Chowdhury *et al.*, (2011); Warshakoon *et al.*, (2006); Chowdhury *et al.*, (2013); Lei *et al.*, (2015); Barrett *et al.*, 2011; Deng *et al.*, (2013) respectively.

1.5.4 Dual-action PHD inhibitors

Yeoh *et al.*, (2013) reported a diacylhydrazine-based dual-action inhibitors that induce the binding of second iron (Fe²⁺) in the PHD-2 active site. Five compounds were identified as potent (<10 μM) among the diacylhydrazine inhibitors. The reported IC₅₀ of values of diacylhydrazine-based dual-action inhibitors are summarized in Table 1.3.

Table 1.3: The IC₅₀ of values of diacylhydrazine-based dual-action PHD inhibitors in PHD-2 active site (Yeoh *et al.*, 2013)

Inhibitor	IC ₅₀ (μM)
	PHD-2
 <p>(3-Pyridyl)fumarate diacylhydrazine</p>	0.082
 <p>(4-Dimethyl-amino-pyridin-2-yl)succinate diacylhydrazine</p>	0.3
 <p>(3-9H-Pyrido[3,4-b]indolyl)succinate diacylhydrazine</p>	0.13
 <p>(3-9H-Pyrido[3,4-b]indolyl)glutarate diacylhydrazine</p>	0.4
 <p>(3-Isoquinolinyl)glutarate diacylhydrazine</p>	9.7

1.6 Therapeutic uses of PHD inhibitors

Utilization of PHD inhibitors to upregulate HIF level is one of the therapeutic indications for ischemic diseases. As mentioned by Soni (2014), small molecule based PHD-2 inhibitors would be a better alternative in treating renal anemia. To date, the roles of PHD-2 inhibitors are proven as an intensive strategy against renal anemia, ischemia and inflammatory diseases (Maxwell and Eckardt. 2016; Gupta and Wish, 2017; Sugahara *et al.*, 2017).

Bernhardt *et al.*, 2006 reported the effect of PHD inhibitor as pharmacological “ischemic preconditioning” agent in activating HIF prior to the right nephrectomy surgery in rat significantly reduces tissue injury and apoptosis. Eckle *et al.*, (2008) also reported the usage of PHD inhibitors before the ischemic/reperfusion (I/R) injury provides strong protection to cardiac tissue and minimizes the extent of myocardial infarct. Furthermore, a study reported by Elena *et al.*, (2011) mentioned that PHD inhibitors also play a crucial role in lowering the ischemic infarct volume and ameliorate ischemic brain injury due to cerebral ischemia. In addition, patients that suffered from severe infectious or ischemic diseases would face one of the persistent complications which is lactic acidosis. A study reported by Suhara *et al.*, (2015) suggested that PHD-2 inhibitors could potentially boost the uptake of lactate for gluconeogenesis and thus resolve the life-threatening lactic acidosis condition. The excessive amounts of lactate release into the circulation is a result of the anaerobic glycolysis, which is the most effective way of produce energy when body cells and tissues are in the demand of oxygen.

PHD inhibitors are also used for the treatment of anemia in patients with chronic kidney disease (CKD). Renal anemia arises from the complication of CKD. When an impaired kidney fails to produce sufficient erythropoietin (EPO), it directly affects the bone marrow in producing fewer red blood cell (RBC) in carrying oxygen throughout

the body. PHD inhibitors have been reported to stimulate erythropoiesis by triggering hypoxic response, stabilizing HIF complex and subsequently activates genes encoding EPO, EPO receptor, transferrin, transferrin receptor, divalent metal transporter 1 (DMT1) copper-carrying protein (ceruloplasmin), and duodenal cytochrome B (Dcytb) (Gupta and Wish, 2017; Provenzano *et al.*, 2016).

Other than that, PHD inhibitors used to elevate HIF levels also found to be a potential treatment for chronic wound healing, especially in elderly or diabetic patients who have reduced capability in HIF expression. In the wound healing process, HIF-1 is crucial in regulating inflammatory and angiogenic responses through the upregulation of HIF-driven transcription gene such as vascular endothelial growth factor (VEGF), nitric oxide synthases, adrenomedullin, metabolic proteins (GLUT-1), soluble growth factors (TGF- β and VEGF) and ECM components (collagen and fibronectin) (Hong *et al.*, 2015; Thangarajah *et al.*, 2009).

1.7 Amide bond and PHD inhibitors

Amide bond formation is well-known as one of the important reactions in organic chemistry. There are three known types of amide: carboxamide, sulfonamide and phosphoramidate. It is a reaction to be reckoned in the pharmaceutical industry due to its high polarity, stability and conformational variety properties in biologically active compounds (Pattabiraman and Bode, 2011).

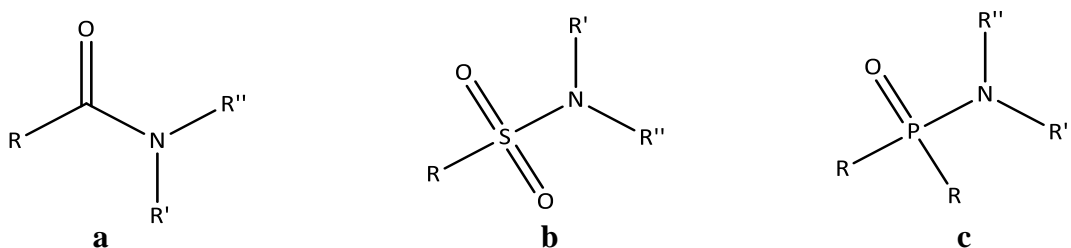
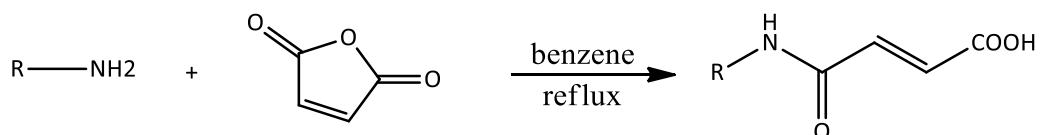


Figure 1.5: Three known types of amide. (a) carboxamide, (b) sulfonamide, (c) phosphoramidate.

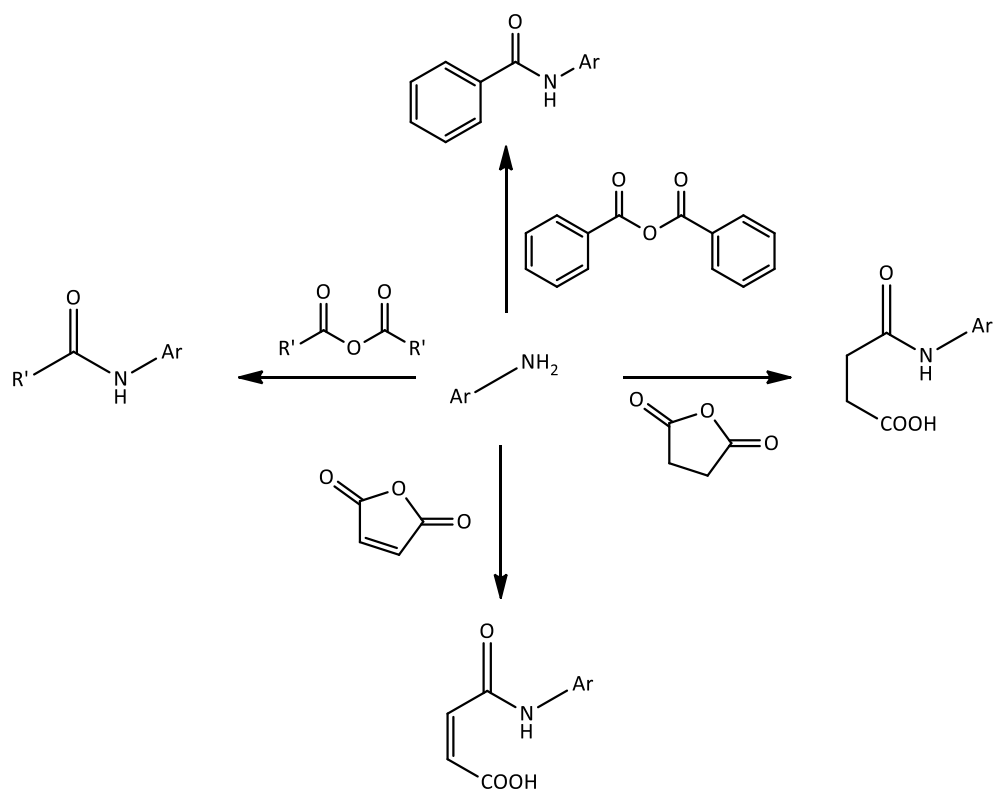
Most of the PHD-2 inhibitors reported consist of carboxamide and sulfonamide which have been identified as one of the crucial functional group contributed to the PHD-2 inhibition. There are many reported methods in generating amide compounds with the presence of catalyst, additives, coupling reagents, organic solvents, acids or bases depends on the substrates used in the reaction scheme.

One of the reaction schemes reported by Omuaru in 1998 in generating carboxamide through the reaction of cyclic anhydrides with aromatic primary amines in the presence of benzene under reflux condition as shown in scheme 1.1.



Scheme 1.1: Reaction of cyclic anhydrides with aromatic primary amines.

The amide reaction scheme was further studied by Naik and colleagues (2004) in which the amines were reacted with cyclic and acyclic anhydride in aqueous media in the presence of sodium dodecyl sulfate (SDS), without acid or base reagents, as shown in Scheme 1.2.



Scheme 1.2: Reaction of cyclic and acyclic anhydrides with amine in aqueous medium.

1.8 Computer Aided Drug Design (CADD)

Herbal remedies were recorded in ancient history, as the only resource for all kinds of medical treatment purposes due to the limitation of synthetic drugs. The emergence of first semi synthetic or synthetic drugs was in the last century with unpromising safety and potency features (Lourenco *et al.*, 2012). Researchers from all over the world spent an outrageous amount and seemingly endless years on discovering a new drug. Every single successfully discovered drug brought to the market could cost up to USD\$800 million to USD\$1.8 billion (Paul *et al.* 2010). Computer Aided Drug Design (CADD) could play an important role in drug discovery field especially in pharmaceutical and biochemistry research. CADD could reduce the overall costing, speeding up the time of bringing lead candidates to market and provide better insight especially in the invincible drug receptor interactions (Hassan *et al.*, 2016).

CADD consists of two major techniques: ligand-based drug design (LBDD) and structure-based drug design (SBDD). The differences between the two techniques are the former one is under the condition where the protein structure is unknown while the latter one is when the three-dimensional structure of target protein is available which can be downloaded at the Protein Data Bank website: www.pdb.com. LBDD utilizes the diverse biological activities information of a series of reported active molecules, overlapping the common features such as hydrophobic, steric or hydrophilic group against the biological targets of interest and hence building up the pharmacophore model (Huang *et al.*, 2010). SBDD utilizes the 3D structure of reported protein as well as the receptor in order to begin the design of potential compounds (Scapin, 2006). The overall progress of discovering drug candidates using CADD is shown in Figure 1.6.

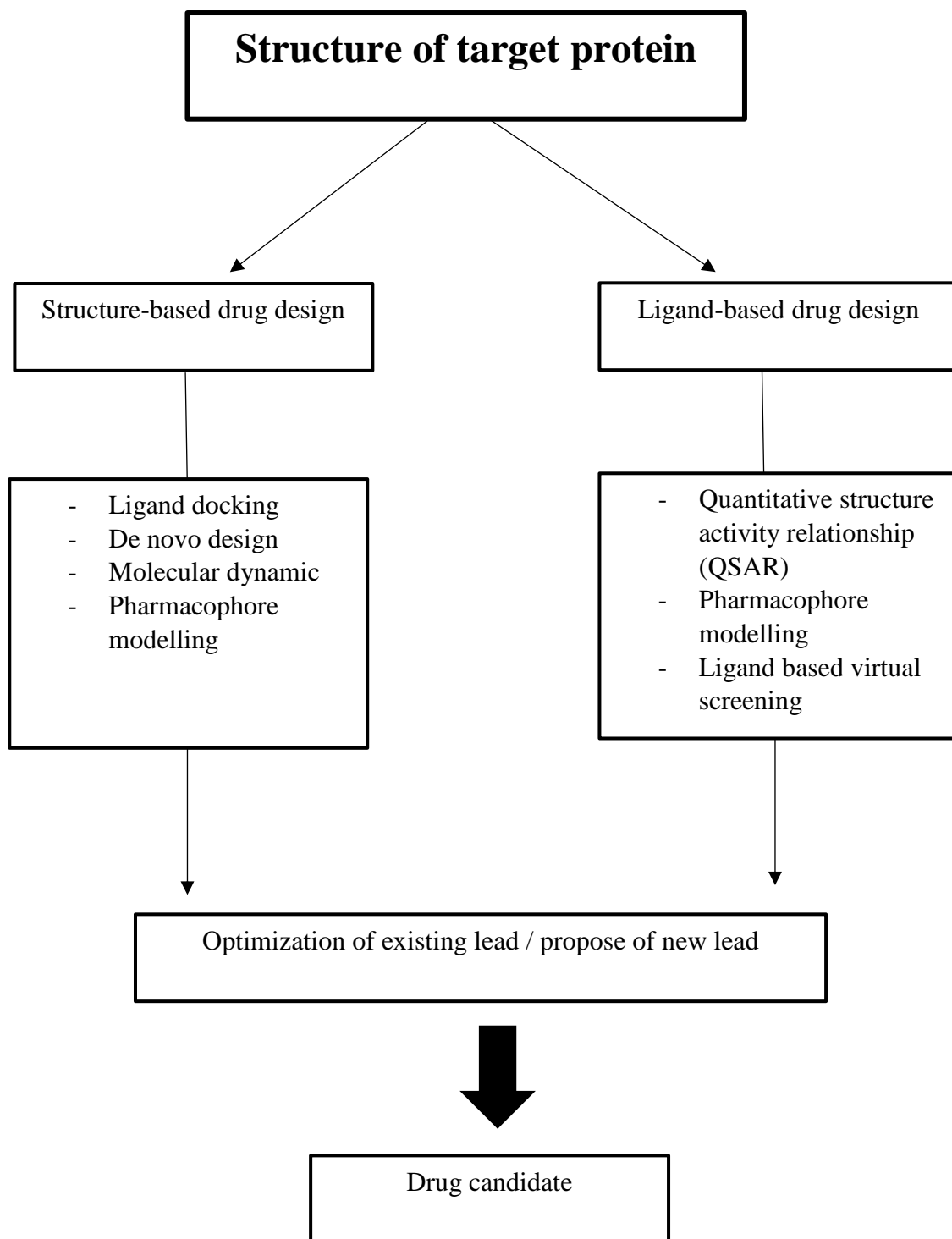


Figure 1.6: The progress of discovering drug candidates using CADD. (Figure adapted from Hassan *et al.*, 2016).

1.9 Problem Statement

Cardiovascular diseases (ischaemic heart disease and stroke) remained on top of the chart as the global diseases over the years, take up the largest percentage of deaths, estimated of 17.5 million (World Health Organization, 2009). Both of these diseases arise from the narrowing of coronary heart arteries due to the formation of fatty deposits (atheroma) and blood clot (thrombosis) in the artery wall, which could partially restricted or totally blocked the flow of oxygenated blood to heart muscle and brain (Davies and Hollman, 2002). These subsequently lead to tissue hypoxia. Without proper and immediate action taken, heart may become permanent damaged and brain cells die within minutes. (Hachinski *et al.*, 2006; Kent *et al.*, 2011). However, when human body facing self-regulation failure in upregulate HIF for adaptive responses, proly hydroxylase domain (PHD) inhibitors play a crucial role in activate the HIF transcriptional activity artificially which have been proven as one of the therapeutic indication for ischemic heart disease and cerebral ischemia (Maxwell and Eckardt. 2016; Gupta and Wish, 2017; Sugahara *et al.* 2017). According to a review done by Yan *et al.*, (2010), most of the PHD inhibitors consisted of two essential functional groups: amide and carboxylic group. Roxadustat (FG4592), Vadadustat (AKB-6548) and Daprodustat (GSK-1278863) that currently undergoing clinical investigation consist of these functional groups. On top of that, Yeoh *et al.*, (2013) also reported that a functionalized bicyclic PHD inhibitors show better inhibitory potency than monocyclic ring.

In this study, a series of 4-oxobutanoic acid analogues that fulfilled the above criterias were tested as potential PHDs inhibitors as well. These compounds were synthesized through the reaction between commercially available amine and succinic anhydride.

1.10 Research Objectives

The research objectives:

1. To design a series of 4-oxobutanoic acid analogues as potential PHD-2 inhibitor using computer aided technique (molecular docking).
2. To synthesize and characterize the synthesized 4-oxobutanoic acid analogues using various spectroscopic methods.
3. To study the inhibitory potencies of 4-oxobutanoic acid analogues.

Scope of study:

This research focuses on the design, synthesis and characterization of 4-oxobutanoic acid analogues as potential HIF prolyl hydroxylase domain-2 (PHD-2) inhibitors. The compounds were designed based on the PHDs inhibitors as reported in literature review. *In silico* computational and molecular docking studies were employed as the following step, guided by Dr Muhd Yusuf from School of Pharmaceutical Sciences to screen over the designed compounds based on their fulfilment of Lipinski's parameter, free energy of binding and binding pose in the active site pocket of PHD-2 crystallographic structure which can be downloaded at www.pdb.com. Compounds which gave positive results in docking studies were further synthesized and characterized using various spectroscopic techniques such as NMR (1D and 2D), mass spectrometry, CHN elemental analysis and FTIR. The inhibitory potencies of 4-Oxobutanoic acid analogue compounds were screened using PHD-2 RapidFire assay which has done by Dr. Martin Abboud in Chemical Research Laboratory, University of Oxford.

CHAPTER 2

MATERIALS AND METHODS

2.1 Chemicals and Solvents

All of the commercial chemicals and reagents that involved in the synthesis were purchased from Sigma-Aldrich, Acros Organics, Fisher Scientific and Maybridge Chemical without further purification. The solvents used: hexane, dichloromethane, ethyl acetate, methanol, tetrahydrofuran, chloroform, anhydrous ethanol and dimethylformamide were all analytical grade from QRċC.

2.2 General Experimental Procedures

2.2.1. Reaction Monitoring

All the reactions were monitored by using the aluminium supported silica gel 60F₂₅₄ thin layer chromatography (TLC) plate (Merck 1.05554.0001). The starting material, reacting reagent, reaction mixture and catalyst (if used) were spotted on the TLC plate, eluted with solvent system of dichloromethane (DCM) and methanol (MeOH) with different ratio. TLC was conducted in a closed glass tank saturated with the vapor of eluent. The spots on the developed TLC plate were then visualized by CAMAG[®] Ultra Violet (UV) Lamp 4 dual wavelength 254nm

2.2.2 Isolation and Purification

2.2.2(a) Column Chromatography

Silica gel 60F, 230-400 mesh ASTM (Merck 1.09385.1000) was used for column chromatography as stationary phase and different organic solvents were used as mobile phase. The silica was first mixed with hexane and formed concoction before it was packed into column. Hexane was loaded continuously in the column for at least one hour before putting samples into the column.

The sample was dry-loaded into the column consisting silica gel and eluted with increasing proportions hexane, DCM as well as MeOH which then formed different fractions of solvent system. The sequence of solvent system eluted in the column chromatography followed the increase in polarity of the chemical solvents. The collected eluent fractions were dried under rotary evaporator and monitor with TLC analysis. Separated components with the same retention factor (R_f) were combined in the same vial.

2.2.2(b) Recrystallization

A single solvent recrystallization was employed for the purification of reaction product. The targeted compound and impurities were completely dissolved in the desired hot solvent. Then the solution slowly cooled to room temperature and allowed to stand for the crystals to grow. The crystals obtained were then filtered by suction filtration. The resulting crystals were then dried in the aspirator.

2.2.3. Characterization of Compounds

All of the synthesized compounds were sent for melting point determination as well as characterization using different spectroscopic methods including Nuclear

Magnetic Resonance (1D and 2D), Fourier Transform Infrared Spectroscopic (FT-IR), mass spectrometry (MS) and elemental analysis.

2.2.3(a) Nuclear Magnetic Resonance Spectroscopy (NMR)

The Nuclear Magnetic Resonance (NMR) spectra of the synthesized compounds were recorded on Bruker Avance spectrometers; 500 MHz for ^1H NMR and 125 MHz for ^{13}C NMR. The 2D spectra included Correlated Spectroscopy (COSY), Heteronuclear Single Quantum Correlation (HSQC) and Heteronuclear Multiple Bond Correlation (HMBC) for the compounds were also recorded on Bruker Avance 500 spectrometer at 500 MHz. Deuterated dimethylsulfoxide (DMSO-d_6) was used to dissolved the samples with tetramethylsilane (TMS) as the internal standard. Chemical shifts (δ) were recorded in part per million (ppm) and coupling constant (J) in Hz.

2.2.3(b) Fourier Transform Infrared Spectroscopy (FT-IR)

All of the synthesized compounds were characterized by Perkin-Elmer 2000 FT-IR spectrometer. A small amount of synthesized compound were grounded into powder form with dry potassium bromide (KBr) in mortar at 1:10 ratio. The mixture powder was then compressed into a thin transparent pellet for the FTIR analysis in the range of 4000 to 400 cm^{-1} .

2.2.3(c) Elemental Analysis

All of the synthesized compounds were analyzed by Perkin Elmer series II, 2400 CHN analyzer by the Science officer of School of Chemical Science, USM.

2.2.3(d) Direct Infusion Mass Spectrometry (DIMS)

All of the synthesized compounds were analyzed by TSQ Quantum TM Access MAX Triple Quadrupole Mass Spectrometer. Samples dissolved in 50/50